Unveiling stability of multiple filamentation caused by axial symmetry breaking of polarization

Si-Min Li,[1] Zhi-Cheng Ren,[1] Ling-Jun Kong,[1] Sheng-Xia Qian,[1] Chenghou Tu,[1,4] Yongnan Li,[1] and Hui-Tian Wang[1,2,3,5]

[1]*MOE Key Laboratory of Weak Light Nonlinear Photonics and School of Physics, Nankai University, Tianjin 300071, China*
[2]*National Laboratory of Solid State Microstructures and School of Physics, Nanjing University, Nanjing 210093, China*
[3]*Collaborative Innovation Center of Advanced Microstructures, Nanjing University, Nanjing 210093, China*
[4]*e-mail: tuchenghou@nankai.edu.cn*
[5]*e-mail: htwang@nju.edu.cn*

Received April 29, 2016; accepted August 6, 2016;
posted August 10, 2016 (Doc. ID 264250); published September 1, 2016

Femtosecond laser filamentation is generally initialized from unpredictable symmetry breaking caused by random noise, causing it to be barely controlled. However, it is always anticipated for stable and controllable filamentation. We present and demonstrate the idea that hybridly polarized vector fields with axial symmetry broken polarization, associated with a pair of orthogonally linearly polarized vortices carrying the opposite-handed orbital angular momenta, could achieve controllable and robust multiple filamentation. Here, our motivation is to unveil the underlying physics behind such controllable and robust multiple filamentation. The symmetry breaking should first be actively controllable and then be able to effectively inhibit random noise. Robust multiple filamentation is inseparable from the fact that the phases between the multiple filaments are always locked. In contrast, uncontrollable multiple filamentation is always accompanied with loss of phase, i.e., the multiple filaments become incoherent to each other. Our results may offer a suggestion for achieving controllable and robust multiple filamentation in other systems.

OCIS codes: (260.5430) Polarization; (260.5950) Self-focusing; (190.3270) Kerr effect; (190.7110) Ultrafast nonlinear optics; (190.3100) Instabilities and chaos; (320.2250) Femtosecond phenomena.
http://dx.doi.org/10.1364/PRJ.4.000B29

1. INTRODUCTION

Field collapse, as a universal phenomenon, has attracted considerable attention; such phenomena occur in most branches of physics. As field collapse exacerbates, other induced nonlinear processes such as higher-order nonlinearity and multiphoton absorption counterbalance the self-focusing effect, preventing further field collapse and resulting ultimately in filamentation. Aside from its unique feature and underlying physics, filamentation becomes a paramount subject due to its various practical applications [1–5]. It should be very helpful to refer to a broad review article for field collapse and the subsequent filamentation [6].

Considerable research has focused on the spatial dynamics and mutual interactions of multiple filaments [7,8]. The field collapse and the subsequent filamentation originate from the self-focusing effect caused by the spatial *inhomogeneity* of the nonlinearity-induced refractive index change. In particular, the multiple filamentation is barely controlled because it is generally initialized by *random* noise of an optical field. However, the actively controlled filamentation is always expected due to the request of various applications. A great challenge is how to tame the randomness. Several approaches such as controlling the input power and divergence angle [9], shaping the field profile [10,11], and using the amplitude/phase mask [12,13] have been proposed. By utilizing the vectorial effect, multiple circularly polarized femtosecond (fs) pulses realized control on two filaments in argon [14], and the linearly polarized field was predicted to result in three filaments [15]. By adjusting the time delay and relative phase, an intense filament could control the position and intensity of a probe filament [16,17]. Theoretical predictions revealed that the phase of the input pulses can control two filaments in air [18,19].

Interestingly, Fibich and Kleinan [20] predicted an effect termed the "loss of phase" in field postcollapse, implying that a postcollapse field can acquire a large accumulative nonlinear phase shift extremely sensitive to a small initial fluctuation through the collapse point. This effect causes the phase of a postcollapse field to become stochastic and the interaction between postcollapse fields becomes chaotic [20]. Two preceding experiments verified that the phase-controlled interaction is robust for precollapse fields but not for postcollapse ones [21,22]. An important experimental advancement [23] confirmed the prediction about the loss-of-phase effect; it also showed that this effect is a universal phenomenon independent of the collapse-arresting mechanisms and that the *loss of relative phases* between postcollapse fields should occur in all systems exhibiting field collapse [23].

Most reports on multiple filamentation have focused on the phase and/or intensity effects for homogeneously polarized fields (HPFs) and polarization vortices during field collapse [15,24–27], whereas the spatial structure of states of polarization (SoPs) was seldomly involved. We have demonstrated controllable and robust field collapse by tailoring the spatial SoP structure of azimuthal-variant hybridly polarized vector

fields (AV-HP-VFs) [28], which are associated with a pair of orthogonally linearly polarized vortices carrying the opposite-handed orbital angular momenta. Such a field collapse has a robust feature against random noise [28].

Some very interesting fundamental questions exist: (i) Is the loss-of-phase effect a universal phenomenon during field collapse? (ii) What is the underlying mechanism behind the loss-of-phase effect? (iii) Can the loss of phase disappear or can stable phase be achieved? (iv) What is the interior relation between the loss of phase and postcollapse (multiple filamentation)? (v) Why is it that the axial symmetry breaking caused by the hybrid SoP structure can result in controllable and robust filamentation? The mission of this paper is to answer these questions.

2. THEORY

In Ref. [28], we focused on the precollapse behavior of the AV-HP-VFs only. As is well known, the self-focusing effect caused by the third-order (Kerr) nonlinearity plays a dominant role in the *precollapse* process. The $(2+1)$-dimensional *vector version* nonlinear Schrödinger equation (NLSE), taking into account the Kerr nonlinearity, is able to simulate the precollapse behavior only [28]. We also proposed a cross-coupling model to intuitively understand the physics behind the precollapse [28]. However, to explore the *postcollapse* (multiple filamentation) behavior of the AV-HP-VFs, we would take into account the contribution of the high-order nonlinearity.

The AV-HP-VFs have an intrinsic difference from HPFs with regard to the field collapse and multiple filamentation. The former originates from the controllable and designable axial symmetry breaking caused by the *hybridly polarized* spatial structure. By contrast, the latter is initialized by the unpredictable axial symmetry breaking caused by the *random noise*. Let us consider a "top-hat-like" profile AV-HP-VF with a field radius of r_0. Such AV-HP-VFs are in fact created by a pair of orthogonally linearly polarized vortex optical fields carrying the opposite-handed orbital angular momenta of $\mp m\hbar$ (where m is the so-called topological charge and $\hbar$ is the reduced Planck's constant being equal to the Planck's constant h divided by 2π), as follows:

$$|\Psi\rangle = E_0\,\mathrm{circ}(\rho/r_0)\{\exp[-j(m\varphi+\varphi_0)](|H\rangle+|V\rangle) + \exp[j(m\varphi+\varphi_0)](|H\rangle-|V\rangle)\}, \tag{1a}$$

$$= 2E_0\,\mathrm{circ}(\rho/r_0)\{\cos(m\varphi+\varphi_0)|H\rangle + \exp(-j\pi/2)\sin(m\varphi+\varphi_0)|V\rangle\}, \tag{1b}$$

where (ρ,φ) indicates the polar coordinate system in the input plane, $\mathrm{circ}(\cdot)$ is the well-known circular function, φ_0 is an initial phase, and $|H\rangle$ and $|V\rangle$ are the horizontally and vertically polarized states, respectively. It is easily proved that under the paraxial condition, for the AV-HP-VF $|\Psi\rangle$ described in Eq. (1), its focal field $|\psi\rangle$ in the focal plane (r,ϕ) is expressed as

$$|\psi\rangle = A_0 Q[\cos(m\phi+\phi_0)|H\rangle + \exp(-j\pi/2)\,\sin(m\phi+\phi_0)|V\rangle], \tag{2}$$

with

$$Q = \frac{(p/2)^m\,{}_1F_2[1+m/2;2+m/2,1+m;-(p/2)^2]}{(m+2)m!},$$

where $\phi_0=\varphi_0$, $p=2\pi r_0 r/\lambda f$, λ is the wavelength of light, f is the focal length of the lens, A_0 is a constant, and ${}_1F_2[]$ is the generalized hypergeometric function.

As is well known, a $(2+1)$-dimensional *scalar-version* NLSE is always used to deal with the collapse and filamentation of an HPF. For an AV-HP-VF, however, we must use a pair of coupled $(2+1)$-dimensional *vector-version* NLSEs, for two orthogonal horizontal and vertical components, as follows:

$$\partial\psi_H/\partial\zeta = (j/4)\nabla_\perp^2\psi_H + jP_H^{(3)} - jP_H^{(5)}, \tag{3a}$$

$$\partial\psi_V/\partial\zeta = (j/4)\nabla_\perp^2\psi_V + jP_V^{(3)} - jP_V^{(5)}, \tag{3b}$$

with

$$P_H^{(3)} = \epsilon' P P_C^{-1}(3|\psi_H|^2\psi_H + 2|\psi_V|^2\psi_H + \psi_V^2\psi_H^*), \tag{4a}$$

$$P_H^{(5)} = \epsilon'' P^2 P_C^{-2}(5|\psi_H|^4\psi_H + 3|\psi_V|^4\psi_H + 2|\psi_V|^2\psi_V^2\psi_H^* + 3|\psi_H|^2\psi_V^2\psi_H^* + \psi_H^3\psi_V^{*2} + 6|\psi_H|^2|\psi_V|^2\psi_H), \tag{4b}$$

where $P_V^{(3)}$ and $P_V^{(5)}$ are easily given provided that the suffixes H and V in the expressions of $P_H^{(3)}$ and $P_H^{(5)}$ are interchanged. $\nabla_\perp^2=\partial^2/\partial\tilde r^2+\tilde r^{-1}\partial/\partial\tilde r+\tilde r^{-2}\partial^2/\partial\phi^2$ is the transverse Laplacian, and $\tilde r=r/r_0$ and $\zeta=z/L_d$ $(L_d=\pi r_0^2/\lambda)$ are the normalized radial vector and normalized propagation distance, respectively. ψ_q $(q=H,V)$ is the complex amplitude normalized by the total field, as $\psi_q=E_q[\iint(|E_H|^2+|E_V|^2)\tilde r\mathrm{d}\tilde r\mathrm{d}\phi]^{-1/2}$, for the q-component. P_C is the critical power for self-focusing and $P=2n_0\varepsilon_0 c\iint(|E_H|^2+|E_V|^2)r\mathrm{d}r\mathrm{d}\phi$ is the input power. ϵ' and ϵ'' describe the third- and fifth-order nonlinearities, respectively.

On the right-hand side of Eq. (3), three terms represent the contributions from the diffraction effect, the Kerr nonlinearity, and the fifth-order nonlinearity, respectively. To explore the precollapse behavior, the third terms on the right-hand side of Eq. (3) can be ignored as in Ref. [28]. To reveal the postcollapse and multiple filamentation, however, we must take into account the contribution of the fifth-order nonlinearity, which is added phenomenologically to counterbalance the self-focusing effect (i.e., to arrest the field collapse) [23].

3. SIMULATIONS

For the focused AV-HP-VF described by Eq. (2), the local linear and circular polarizations are located at azimuthal angles $\phi^{\mathrm{lin}}(n)=n\pi/2m-\phi_0/m$ and $\phi^{\mathrm{cir}}(n)=(2n+1)\pi/4m-\phi_0/m$ (where $n=0,1,\ldots,4m-1$), respectively, and the local SoPs are elliptically polarized elsewhere.

Figure 1(a) shows the intensity and SoP distributions of the focused AV-HP-VF with $m=2$ and $\phi_0=0$, which exhibits a focal ring, although a spatial randomly distributed noise with a $\pm10\%$ amplitude has been added. The simulation results in Figs. 1(b)–1(f) are given under the conditions of $P=12P_C$, $\zeta=1.6$, $\epsilon'=0.33$, and $\epsilon''=10^{-4}$, with the spatial randomly distributed noise of a $\pm10\%$ amplitude. As shown in Fig. 1(b), the focused AV-HP-VF in Fig. 1(a) collapses to

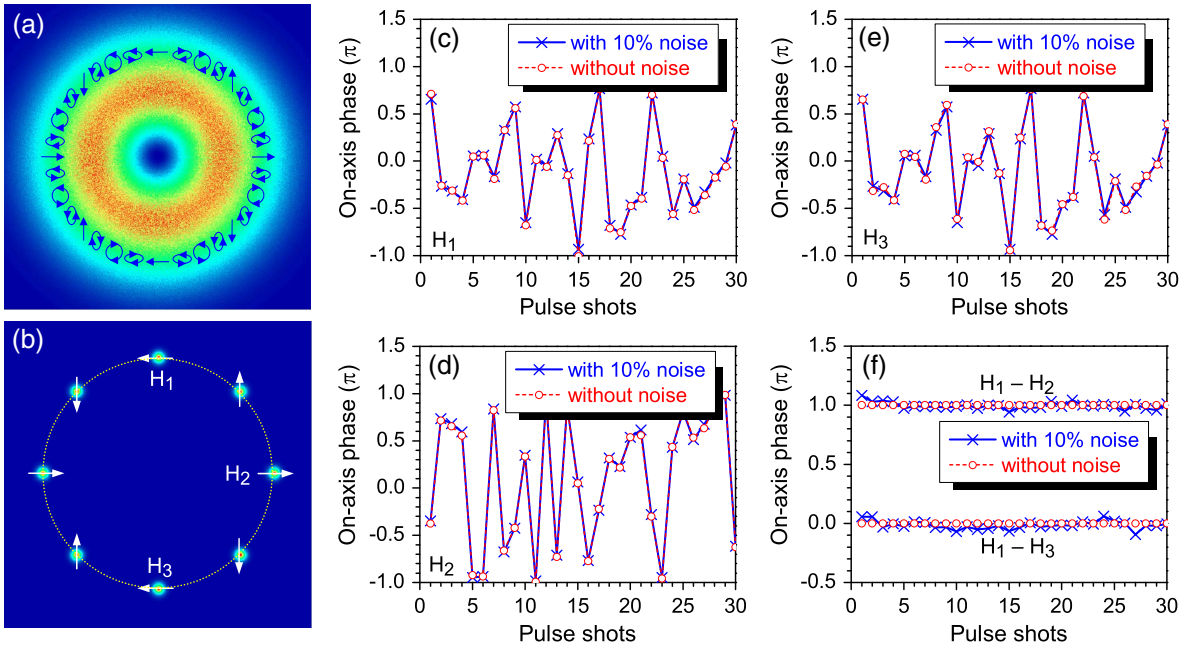

Fig. 1. (a) Simulated intensity pattern and SoP distribution of the focused AV-HP-VF with $m = 2$ and $\phi_0 = 0$, and 10% amplitude random noise. (b) Simulated filamentation pattern of the AV-HP-VF shown in (a) under the conditions of $P = 12P_C$, $\zeta = 1.6$, $\epsilon' = 0.33$, and $\epsilon'' = 10^{-4}$. (c)–(e) Simulated on-axis accumulated phases for three filaments labeled H_1, H_2, and H_3 under the same conditions as (b). (f) Simulated relative phases between H_1 and H_2 as well as H_1 and H_3. For comparison, the simulated on-axis phases of the perfect AV-HP-VF with $m = 2$ and $\phi_0 = 0$ are given in (c)–(f).

converge toward a distinct profile composed of eight filaments, which are homogeneously distributed in a circle. This suggests that the random noise has no significant effect on the multiple filamentation pattern. Unlike the HPFs, the random noise does not serve as a seed for the field collapse. We also confirm that the SoPs of multiple filaments are linearly polarized and in good agreement with those of the focused AV-HP-VF in Fig. 1(a). As shown in Figs. 1(c)–1(e), the calculated on-axis accumulated phase shifts of three filaments (H_1, H_2, and H_3) have uncertainty, that is to say, the phase of any individual filament still exhibits the loss-of-phase effect as reported in Refs. [23,29,30]. Unlike the HPFs, however, the *relative phases* between the multiple filaments are always *robust*. As shown in Fig. 1(f), the relative phase between H_1 and H_2 (H_1 and H_3) is always in phase (out of phase). For the focused AV-HP-VF shown in Fig. 1(a) at the azimuthal angles corresponding to H_1 and H_2 (H_1 and H_3), the linear polarizations are also parallel (antiparallel), which is equivalent to being in phase (out of phase). For comparison, the postcollapse phase behaviors of the perfect AV-HP-VFs are also shown in Figs. 1(c)–1(f).

Aside from the random noise, the energy fluctuation between successive pulses may affect the field collapse and multiple filamentation. To further understand the collapsing evolution and multiple filamentation of the AV-HP-VF, we explore the dependence of the peak intensity of the filament on the propagation distance at different random noise levels, as shown in Fig. 2(a). After the first collapse point occurs at $\zeta = 0.75$, the filament undergoes the focusing–defocusing oscillation. Numerous simulations for various different random noises in both amplitude and phase reveal that the random noise has no almost effect on the peak intensity of the filaments. As shown in Fig. 2(b), the higher pulse power results in shorter collapsing distance and higher intensity at the collapse points. However, this kind of energy fluctuation between successive pulses has no effect on the relative power between filaments.

To illustrate the collapsing evolution and multiple filamentation of the AV-HP-VFs in a Kerr medium, Fig. 3 shows the simulation results of two AV-HP-VFs with $m = 1$ and $m = 2$ when $\epsilon' = 0.33$, $\epsilon'' = 10^{-4}$, and $P = 12P_C$ (a 10% amplitude noise is added for two simulations). Beyond the collapse point, the sizes and the intensity of the filaments experience synchronous oscillations with the propagation distance. The added random noise has almost no influence on the filamentation patterns and the filaments in the output face of the nonlinear medium are positioned in a circle, like the perfect AV-HP-VF. The AV-HP-VF with the larger m quickly collapses and then converges to the filaments. This phenomenon is easily understood by using the azimuthal self-focusing model. In a Kerr medium, the induced refractive index change Δn depends on the SoP of the optical field, with $\Delta n^{\mathrm{lin}} > \Delta n^{\mathrm{ell}} > \Delta n^{\mathrm{cir}}$ ($\Delta n^{\mathrm{lin}} = 1.5\Delta n^{\mathrm{cir}}$). For the AV-HP-VF, because its SoPs exhibit azimuthal periodicity from linear polarization to a circular one through the elliptic one, Δn is a periodic function of ϕ within a range from Δn^{cir} to Δn^{lin}, which serves as an azimuthally arranged self-focusing lens. An AV-HP-VF with the topological charge m will induce $4m$ azimuthal self-focusing lenses. Given that $\Delta n^{\mathrm{lin}} - \Delta n^{\mathrm{cir}}$ is fixed under the same input conditions, the azimuthal self-focusing lenses induced by the AV-HP-VF with a larger m should have the shorter focal length. Thus, the AV-HP-VF with the larger m has the shorter collapsing distance.

As mentioned previously, the field collapse and multiple filamentation of the AV-HP-VF are controllable, predictable, and designable by engineering the spatial structure of hybrid SoPs.

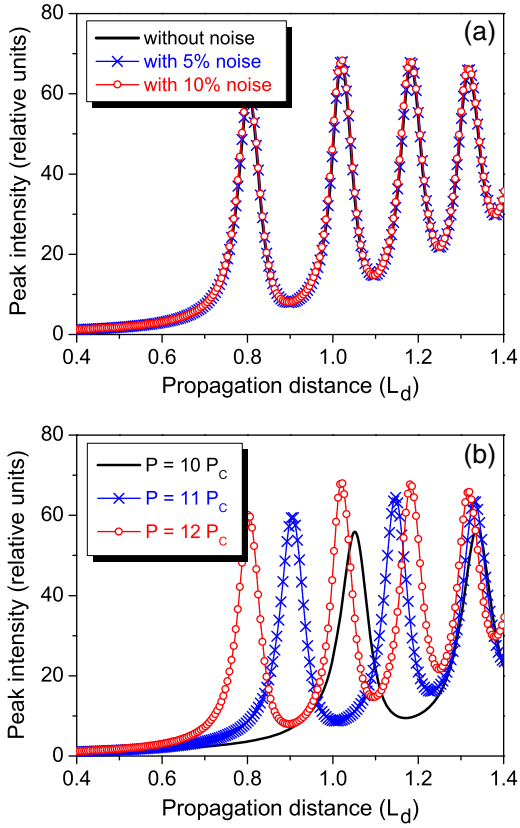

Fig. 2. Simulated evolution of the peak intensity of filament with the propagation distance for AV-HP-VF with $m = 2$ and $\phi_0 = 0$, under the conditions of $\epsilon' = 0.33$ and $\epsilon'' = 10^{-4}$ (a) at different random noise levels of no noise, 5% noise, and 10% noise at $P = 12P_C$ and (b) at different input powers of $P = 10P_C$, $11P_C$, and $12P_C$ without random noise.

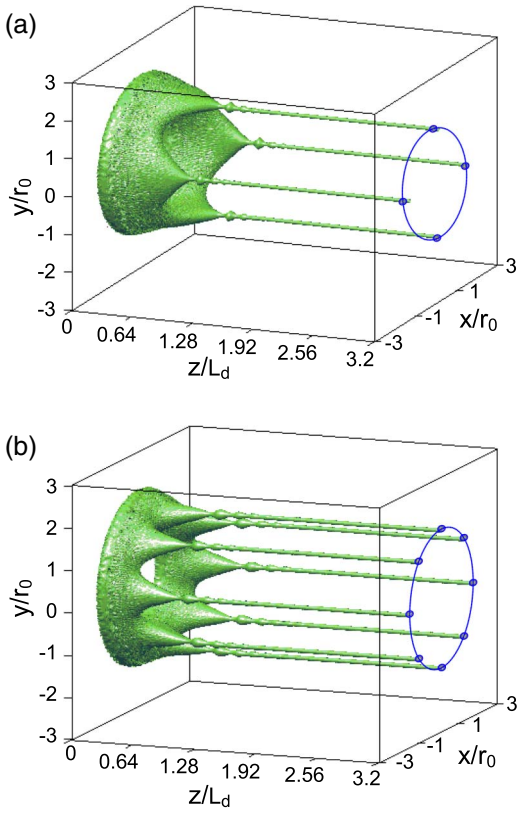

Fig. 3. Simulated collapsing evolution and multiple filamentation of the AV-HP-VFs by Eq. (3) under the conditions of $\epsilon' = 0.33$, $\epsilon'' = 10^{-4}$, and $P = 12P_C$ with 10% amplitude random noise. (a) AV-HP-VF with $m = 1$ and $\phi_0 = 0$. (b) AV-HP-VF with $m = 2$ and $\phi_0 = 0$.

In particular, the multiple filamentation has a robust feature insensitive to the random noise. The relative phases between filaments are robust regardless of any individual filament exhibiting the loss-of-phase phenomena (its phase shift has a dramatic change). Other simulation results (not shown here) demonstrate the following facts. For the AV-HP-VF with the spatial randomly distributed noise, the filamentation patterns become unpredictable or random, and the loss-of-phase phenomena also occurs when the random noise and/or pulse energy have higher levels. In this situation, the competition results in the random noise becoming dominant as the seed for the field collapse instead of the spatial SoP distribution.

4. EXPERIMENTAL RESULTS

To verify our prediction, we perform experiments on the field collapse and multiple filamentation of the AV-HP-VFs, which are created by a scheme similar to that in Refs. [31,32]. A Ti:sapphire fs regenerative amplifier as a light source has a pulse duration of ~35 fs, operating at a repetition rate of 1 kHz and a central wavelength of 800 nm. The created AV-HP-VFs with topological charge m and initial phase φ_0 have a "top-hat-like" spatial profile, excluding a central polarization singularity, with diameter of $r_0 = 3.0$ mm, maximum pulse energy of 6.0 μJ, and pulse duration of ~65 fs. The focused AV-HP-VF by an achromatic lens with $f = 60$ mm is incident into a CS_2 (as a Kerr medium) cell with a length of 10 mm. The input face of the cell is located in the vicinity of focal plane of the lens. The intensity patterns of the multiple filaments from the output face of the cell are recorded by imaging them onto a CCD detector.

Figure 4 shows the measured six consecutive, 10-shot-average CCD images of the filamentation patterns at the output face of the cell, produced by two AV-HP-VFs with $m = 1$ and $m = 2$ at a pulse energy of 2.0 μJ. Clearly, the two AV-HP-VFs collapse into the stable four and eight filaments, respectively. The measured filamentation patterns and the SoPs of filaments are in good agreement with the just-discussed theoretical predictions. Very importantly, the experimental results confirm that the multiple filamentation patterns produced by the two AV-HP-VFs are stable when the input pulse energy is within a range from 1.4 to 2.7 μJ. When the pulse energy exceeds 2.7 μJ, however, the output pattern becomes unstable like the traditional filamentation initialized by the random noise, which is easily understood below. Due to the competition between the spatial symmetry breakings caused by the random noise and hybrid SoPs, the former is dominant when the pulse energy exceeds a certain critical level, whereas the latter is dominant because the former is inhibited when the pulse energy is lower than the critical level. So long as the pulse energy is limited within a suitable range, the multiple filamentation can be well controlled by engineering the spatial SoP structure. In fact, this energy range, which ensures the stable multiple filamentation pattern, is not so narrow, and we can even say the range is quite broad. If the AV-HP-VF propagates in atmosphere, the energy range for stable filamentation will be broadened dramatically because the

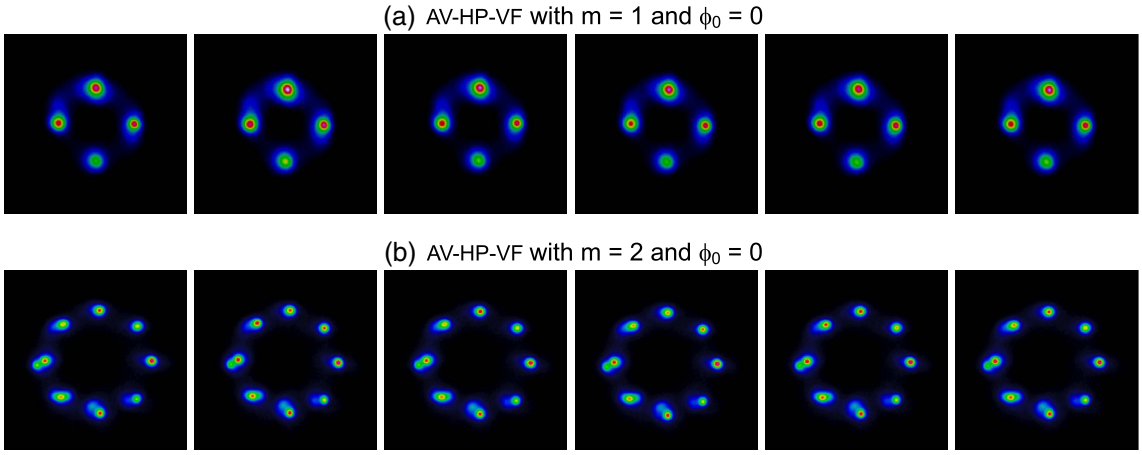

Fig. 4. Measured six consecutive, 10-shot average CCD images of filamentation of AV-HP-VFs at 2.0 μJ pulse energy for two AV-HP-VFs with (a) $m = 1$ and (b) $m = 2$.

nonlinearity of atmosphere is much lower than that of the CS_2 used in this work.

Unlike the HPFs, the cross-coupling between two orthogonally polarized components carrying the opposite-handed orbital angular momenta plays an irreplaceable role in the field collapse and multiple filamentation of the AV-HP-VF. The cross coupling causes the energy of a linearly polarized component of the circularly/elliptically polarized light to be irreversibly exchanged into another orthogonally polarized one due to the presence of a phase difference $\pi/2$ between the two orthogonally polarized components. Thus, the circularly/elliptically polarized light trends to become the linearly polarized one. The combination of cross coupling and azimuthal self-focusing effect results finally in deterministic filaments. We have thus confirmed theoretically and experimentally that postcollapse interactions can be robust and insensitive to input fluctuation (i.e., the loss of relative phase does not occur), because the collapse of the AV-HP-VF is not initialized by the random noise.

5. CONCLUSION

In summary, we investigated the stability of multiple filamentation caused by the axial symmetry breaking of polarization. The AV-HP-VFs with axial symmetry breaking of polarization are created by the combination of a pair of orthogonally linearly polarized vortices carrying the opposite-handed orbital angular momenta. We use the vector version NLSE, including the quintic nonlinearity, to simulate the field-collapsing evolution of the AV-HP-VFs, including the precollapse and postcollapse (multiple filamentation).

For the HPFs, the accumulated phase of any individual filament and the relative accumulated phases between any two filaments are unpredictable (loss-of-phase), that is to say, the filaments are incoherent each other. As a result, the instabilty of field collapse and multiple filamentation always accompany the loss-of-phase effect. In contrast, for the AV-HP-VFs, althrough the accumulated phase of any individual filament has uncertainty or suffers from the loss-of-phase effect, the *relative phases* between any two deterministic filaments *are always locked* (in other words, all the filaments are *coherent to each other*). Therefore, the underlying mechanism behind the stability of multiple filamentation should be the *locked-relative phase*. The loss-of-phase effect for any individual filament should be a universal phenomenon, whereas the locked-relative phase should not be a universal phenomenon. Since the random noise is always hard to avoid and the field collapse is generally initialized from the unpredictable symmetry breaking caused by the random noise, to achieve the desired multiple filamentation, the symmetry breaking should not only be controllable and realizable, but also be able to suppress the unpredictable random symmetry breaking. The locked-relative phase coexists always with the controllable and robust multiple filamentation initialized from the effectively active symmetry breaking, while the loss-of-relative-phase effect is closely related to the multiple filamentation initialized from the symmetry breaking caused by the random noise. We believe that the controllable and designable spatial structures of polarization should be applied more comprehensively in many branches of physics.

Funding. 973 Program of China (2012CB921900); National Natural Science Foundation of China (NSFC) (11274183, 11374166, 11504409, 11534006); National Scientific Instrument and Equipment Development Project (2012YQ17004); Collaborative Innovation Center of Extreme Optics.

REFERENCES

1. J. Kasparian, M. Rodriguez, G. Méjean, J. Yu, E. Salmon, H. Wille, R. Bourayou, S. Frey, Y. B. André, A. Mysyrowicz, R. Sauerbrey, J. P. Wolf, and L. Wöste, "White-light filaments for atmospheric analysis," Science **301**, 61–64 (2003).
2. P. Rohwetter, J. Kasparian, K. Stelmaszczyk, Z. Q. Hao, S. Henin, N. Lascoux, W. M. Nakaema, Y. Petit, M. Queißer, R. Salamé, E. Salmon, L. Wöste, and J. P. Wolf, "Laser-induced water condensation in air," Nat. Photonics **4**, 451–456 (2010).
3. F. Belgiorno, S. L. Cacciatori, M. Clerici, V. Gorini, G. Ortenzi, L. Rizzi, E. Rubino, V. G. Sala, and D. Faccio, "Hawking radiation from ultrashort laser pulse filaments," Phys. Rev. Lett. **105**, 203901 (2010).
4. C. D'Amico, A. Houard, M. Franco, B. Prade, and A. Mysyrowicz, "Conical forward THz emission from femtosecond-laser-beam filamentation in air," Phys. Rev. Lett. **98**, 235002 (2007).
5. C. P. Hauri, W. Kornelis, F. W. Heibing, A. Heinrich, A. Couairon, A. Mysyrowicz, J. Biegert, and U. Keller, "Generation of intense, carrier-envelope phase-locked few-cycle laser pulses through filamentation," Appl. Phys. B **79**, 673–677 (2004).

6. A. Couairon and A. Mysyrowicz, "Femtosecond filamentation in transparent media," Phys. Rep. **441**, 47–189 (2007).
7. S. Tzortzakis, L. Bergé, A. Couairon, M. Franco, B. Prade, and A. Mysyrowicz, "Breakup and fusion of self-guided femtosecond light pulses in air," Phys. Rev. Lett. **86**, 5470–5473 (2001).
8. S. A. Hosseini, Q. Luo, B. Ferland, W. Liu, S. L. Chin, O. G. Kosareva, N. A. Panov, N. Aközbek, and V. P. Kandidov, "Competition of multiple filaments during the propagation of intense femtosecond laser pulses," Phys. Rev. A **70**, 033802 (2004).
9. Z. Jin, J. Zhang, M. H. Xu, X. Lu, Y. T. Li, Z. H. Wang, Z. Y. Wei, X. H. Yuan, and W. Yu, "Control of filamentation induced by femtosecond laser pulses propagating in air," Opt. Express **13**, 10424–10430 (2005).
10. A. Dubietis, G. Tamošauskas, G. Fibich, and B. Ilan, "Multiple filamentation induced by input-beam ellipticity," Opt. Lett. **29**, 1126–1128 (2004).
11. T. D. Grow and A. L. Gaeta, "Dependence of multiple filamentation on beam ellipticity," Opt. Express **13**, 4594–4599 (2005).
12. T. Pfeifer, L. Gallmann, M. J. Abel, D. M. Neumark, and S. R. Leone, "Circular phase mask for control and stabilization of single optical filaments," Opt. Lett. **31**, 2326–2328 (2006).
13. Z. Q. Hao, K. Stelmaszczyk, P. Rohwetter, W. M. Nakaema, and L. Woeste, "Femtosecond laser filament-fringes in fused silica," Opt. Express **19**, 7799–7806 (2011).
14. A. Trisorio and C. P. Hauri, "Control and characterization of multiple circularly polarized femtosecond filaments in argon," Opt. Lett. **32**, 1650–1652 (2007).
15. G. Fibich and B. Ilan, "Deterministic vectorial effects lead to multiple filamentation," Opt. Lett. **26**, 840–842 (2001).
16. S. Varma, Y. H. Chen, and H. M. Milchberg, "Trapping and destruction of long-range high-intensity optical filaments by molecular quantum wakes in air," Phys. Rev. Lett. **101**, 205001 (2008).
17. F. Calegari, C. Vozzi, S. Gasilov, E. Benedetti, G. Sansone, M. Nisoli, S. De Silvestri, and S. Stagira, "Rotational Raman effects in the wake of optical filamentation," Phys. Rev. Lett. **100**, 123006 (2008).
18. L. Bergé, M. R. Schmidt, J. Juul Rasmussen, P. L. Christiansen, and K. Ø. Rasmussen, "Amalgamation of interacting light beamlets in Kerr-type," J. Opt. Soc. Am. B **14**, 2550–2562 (1997).
19. T. T. Xi, X. Lu, and J. Zhang, "Interaction of light filaments generated by femtosecond laser pulses in air," Phys. Rev. Lett. **96**, 025003 (2006).
20. G. Fibich and M. Klein, "Continuations of the nonlinear Schrödinger equation beyond the singularity," Nonlinearity **24**, 2003–2045 (2011).
21. A. A. Ishaaya, T. D. Grow, S. Ghosh, L. T. Vuong, and A. L. Gaeta, "Self-focusing dynamics of coupled optical beams," Phys. Rev. A **75**, 023813 (2007).
22. B. Shim, S. E. Schrauth, C. J. Hensley, L. T. Vuong, P. Hui, A. A. Ishaaya, and A. L. Gaeta, "Controlled interactions of femtosecond light filaments in air," Phys. Rev. A **81**, 061803 (2010).
23. B. Shim, S. E. Schrauth, A. L. Gaeta, M. Klein, and G. Fibich, "Loss of phase of collapsing beams," Phys. Rev. Lett. **108**, 043902 (2012).
24. L. T. Vuong, T. D. Grow, A. Ishaaya, A. L. Gaeta, G. W. 't Hooft, E. R. Eliel, and G. Fibich, "Collapse of optical vortices," Phys. Rev. Lett. **96**, 133901 (2006).
25. A. A. Ishaaya, L. T. Vuong, T. D. Grow, and A. L. Gaeta, "Self-focusing dynamics of polarization vortices in Kerr media," Opt. Lett. **33**, 13–15 (2008).
26. T. D. Grow, A. A. Ishaaya, L. T. Vuong, and A. L. Gaeta, "Collapse and stability of necklace beams in Kerr media," Phys. Rev. Lett. **99**, 133902 (2007).
27. G. Fibich and B. Ilan, "Multiple filamentation of circularly polarized beams," Phys. Rev. Lett. **89**, 013901 (2002).
28. S. M. Li, Y. N. Li, X. L. Wang, L. J. Kong, K. Lou, C. H. Tu, Y. J. Tian, and H. T. Wang, "Taming the collapse of optical fields," Sci. Rep. **2**, 1007 (2012).
29. M. Mlejnek, M. Kolesik, J. V. Moloney, and E. M. Wright, "Optically turbulent femtosecond light guide in air," Phys. Rev. Lett. **83**, 2938–2941 (1999).
30. L. Bergé, S. Skupin, F. Lederer, G. Méjean, J. Yu, J. Kasparian, E. Salmon, J. P. Wolf, M. Rodriguez, L. Wöste, R. Bourayou, and R. Sauerbrey, "Multiple filamentation of terawatt laser pulses in air," Phys. Rev. Lett. **92**, 225002 (2004).
31. X. L. Wang, J. P. Ding, W. J. Ni, C. S. Guo, and H. T. Wang, "Generation of arbitrary vector beams with a spatial light modulator, a common path interferometric arrangement," Opt. Lett. **32**, 3549–3551 (2007).
32. X. L. Wang, Y. N. Li, J. Chen, C. S. Guo, J. P. Ding, and H. T. Wang, "A new type of vector fields with hybrid states of polarization," Opt. Express **18**, 10786–10795 (2010).